

Article ID: 1006-8775(2012) 01-0001-10

## A STUDY ON THE PRECIPITATION CHARACTERISTICS OVER THE SOUTH CHINA SEA BEFORE AND AFTER THE MONSOON ONSET

LI Yao-dong (李耀东)<sup>1</sup>, SONG Ming-kun (宋明坤)<sup>1,2</sup>, HU Liang (胡亮)<sup>3</sup>

(1. Institute of Aviation Meteorology, Beijing 100085 China; 2. Institute of Meteorology, PLA University of Science and Technology, Nanjing 211101 China; 3. National Satellite Meteorology Center, CMA, Beijing 100081 China)

**Abstract:** This paper presents a study on the temporal and spatial variations of the precipitation over the area of the South China Sea (SCS) during the monsoon onset period. The data used are from the Tropical Rainfall Measuring Mission (TRMM) observations between April and June over the nine years from 1998 to 2006. This study focuses on the central and northern part of South China Sea (110–120°E, 10–20°N). Based on the observations, the 27th pentad is selected as the occurrence time of the SCS monsoon onset. The conclusions are as follows. (1) After the monsoon onset, the specific area, defined as the ratio of the number of pixels with certain type of precipitation to the number of total pixels, extends significantly for both convective and stratiform rain, with the latter having a larger magnitude. The specific rainfall, defined as the ratio of the amount of certain type of precipitation to the total amount of precipitation, decreases for convective rain and increases for stratiform rain. (2) Results also show significant increase in heavy rain and decrease in light rain after the monsoon onset. (3) Changes are also observed in the rainfall horizontal distributions over the SCS before and after the monsoon onset, manifested by the relocation of precipitation minima for both convective and stratiform rain. (4) After the monsoon onset, the variability in characteristics of precipitation vertical structure increases significantly, leading to more latent heat release and consequently deeper convection. Meanwhile, the bright-band altitude of stratiform precipitation is also elevated.

**Key words:** TRMM; South China Sea; monsoon onset; precipitation

**CLC number:** P426.6

**Document code:** A

**doi:** 10.3969/j.issn.1006-8775.2012.01.001

### 1 INTRODUCTION

As part of the tropical Pacific, the SCS is surrounded by the mainland of China to its north, the Indonesian archipelago to its south, the Philippines to its east and the Indochina Peninsula to its west. Geographically, SCS is the linkage between the North Pacific Ocean and the North Indian Ocean. Over this region, the wind patterns demonstrate clear summer and winter monsoon features. Consequently, monsoon activities have significant impact on the weather pattern over the SCS. Furthermore, as the origin of the East Asia monsoon, the SCS monsoon plays a critical role in determining the distribution of summer precipitation over China via the time of onset and the strength of the system, and thus directly affects the development of the East Asian summer monsoon<sup>[1-3]</sup>. Lau et al.<sup>[4]</sup> have shown that precipitation and latent heat release over the SCS have significant impact on

the atmospheric circulation and energy budget over the East Asian region.

Horizontally, the distribution of precipitation strength at the surface can be observed from space, as it reflects the properties of the precipitating cloud clusters to a certain extent<sup>[5]</sup>. Vertically, the structure of precipitation reflects the thermodynamics and kinetics of the precipitating clouds and their microphysical properties<sup>[6-8]</sup>. Houze<sup>[9]</sup> showed that because of the differences in vertical structure, different types of precipitation result in different heating structure in the vertical direction. For example, latent heat released from the stratiform rainfall is mainly located at the upper troposphere, while that from the convective rainfall spreads across the entire troposphere. Hence, investigating the precipitation characteristics over the SCS before and after monsoon onset is important to further understanding of the SCS summer monsoon circulation system.

**Received** 2010-11-08; **Revised** 2011-12-22; **Accepted** 2012-01-15

**Foundation item:** National Science Foundation of China (41175046)

**Biography:** LI Yao-dong, senior engineer, mainly undertaking research on numerical weather prediction and application of meteorological satellite data.

**Corresponding author:** LI Yao-dong, e-mail: lyd@mail.iap.ac.cn

In recent years, numerous studies have been conducted on the SCS monsoon precipitation with data from the South China Sea Monsoon Experiment (SCSMEX) as well as satellites. For example, using data obtained from the SCS Experiment on Ocean-Atmosphere Fluxes, the US National Centers for Environmental Prediction (NCEP), the Global Precipitation Climatology Project (GPCP) and GMS-5 satellite observations, Yan et al.<sup>[10]</sup> conducted a detailed study on the variation of the Central and East Asia rain belts during the genesis of the SCS southwest monsoon. They found that at the monsoon onset, the precipitation pattern is featured by a single rain belt, which then turns into double belts. The rain belts are simultaneously affected by the subtropical high and monsoon system, e.g., their locations change with the movement of the subtropical high. Jiang et al.<sup>[11]</sup> studied the spatial and temporal distribution of the precipitation over the SCS region with wavelet analysis. Their results showed that the SCS region can be divided into three areas: the northern area (20–22°N), the central area (110–120°E, 10–20°N) and the southern area (<10°N). Precipitation mainly occurs within the northern and central areas. Within the northern area, the precipitation shows a single mode with stable enhancement; within the central area, the variability of precipitation is more abrupt and larger during the rain season. Liu et al.<sup>[12]</sup> investigated the monsoon onset characteristics in the northern area of the SCS with data from SCSMEX. They demonstrated that the establishment of the SCS monsoon trough and the low-level shear as well as the occurrence and development of the associated mesoscale vortex are prerequisite for the formation and persistence of the mesoscale convective systems. However, even though numerous studies have been conducted on the SCS monsoon, existing literature mainly focuses on the characteristics of the rain belt variation before and after the monsoon onset. The analysis is quite little on the horizontal and vertical structure of different precipitation types during the monsoon onset.

Launched on 27 November 1997, TRMM has been providing invaluable data for studying the horizontal distribution and vertical structure of tropical precipitation. With the TRMM 2A25 data collected during April to June, 1998 to 2006, this paper presents an analysis on the differences in horizontal distribution and vertical structure of precipitation before and after the monsoon onset. The impact of the SCS monsoon on the precipitation of this region is also discussed.

## 2 DATA AND METHODOLOGY

The TRMM Precipitation Radar (PR) was the first spaceborne active remote sensing instrument designed

to provide three-dimensional precipitation structure. The TRMM 2A25-retrieved three-dimensional rain rate (mm/h) provides the vertical profile of precipitation with a horizontal resolution of 5 km (4.3 km before the increase of orbit altitude) and a vertical resolution of 250 m. Data with such a high resolution is critical to studying tropical precipitation. In addition, TRMM 2A25 also provides information on precipitation type. The rain type parameter categorizes precipitation into three types: convective, stratiform and other. As the type “other” accounts for only a very small percentage<sup>[13]</sup>, hence in this paper, our investigation only focuses on the stratiform and convective rain types. Considering the sensitivity of PR, we only take into account rain rates above 0.5 mm/h. To avoid ground clutters, the starting height for the precipitation contours is set at 2 km.

Usually, the most evident monsoon-related seasonal changes are observed during the period of late April to early June (19th pentad to 36th pentad) over the SCS region<sup>[14]</sup>, which is therefore used for the analysis of precipitation features in this study. Table 1 gives the total number of samples (i.e. the total number of TRMM pixels), and the sample number for convective and stratiform rainfall for each pentad from April to June.

Table 1 shows that the total number of samples for different pentads are slightly different, which could cause small biases to the results. To solve this problem, smoothing is applied to the number of pixels and the amount of precipitation, which are multiplied by ratios between the average of samples of all pentads and the total number of samples of this pentad. In doing so, we get the same number of samples for every pentad.

Table 1. Number of precipitation pixels observed by TRMM over the SCS. The shaded values are for the time after the monsoon onset.

	Total	Convective	Stratiform	
April	19 <sup>th</sup> pentad	912 960	3 378	4 983
	20 <sup>th</sup> pentad	944 677	4 960	8 273
	21 <sup>st</sup> pentad	912 905	4 606	4 386
	22 <sup>nd</sup> pentad	928 997	5 205	5 744
	23 <sup>rd</sup> pentad	943 188	2 590	2 457
	24 <sup>th</sup> pentad	920 374	7 679	20 900
May	25 <sup>th</sup> pentad	917 302	4 465	4 457
	26 <sup>th</sup> pentad	946 305	7 982	15 210
	27 <sup>th</sup> pentad	898 398	14 801	35 990
	28 <sup>th</sup> pentad	934 697	14 210	34 529
	29 <sup>th</sup> pentad	926 981	19 879	53 558
	30 <sup>th</sup> pentad	915 833	17 986	49 077
June	31 <sup>st</sup> pentad	935 510	16 822	46 712
	32 <sup>nd</sup> pentad	910 586	12 659	36 530
	33 <sup>rd</sup> pentad	927 880	10 420	24 249
	34 <sup>th</sup> pentad	938 192	13 590	34 819
	35 <sup>th</sup> pentad	891 592	13 926	34 761
	36 <sup>th</sup> pentad	937 313	17 594	59 621

## 3 SELECTION OF RESEARCH AREA AND DETERMINATION OF THE MONSOON

## ONSET DATE

### 3.1 Selection of research area

One major signature of the SCS monsoon onset is the rapid development and enhancement in convective activities and convective precipitation<sup>[15, 16]</sup>. Many studies have demonstrated that usually the SCS monsoon onset occurs during mid-May when the regional precipitation shows abrupt change<sup>[17-21]</sup>. This change is most obvious over the central and northern

part of South China Sea (110–120°E, 10–20°N). Figures 1 and 2 give the horizontal distributions of average convective and stratiform rain rates for each pentad of May. As shown in the figures, although the convective rain rate is always larger than the corresponding stratiform rain rate over the entire region, the most evident change during this period occurs over the region denoted by the dashed lines (110–120°E, 10–20°N), which is selected for the study.

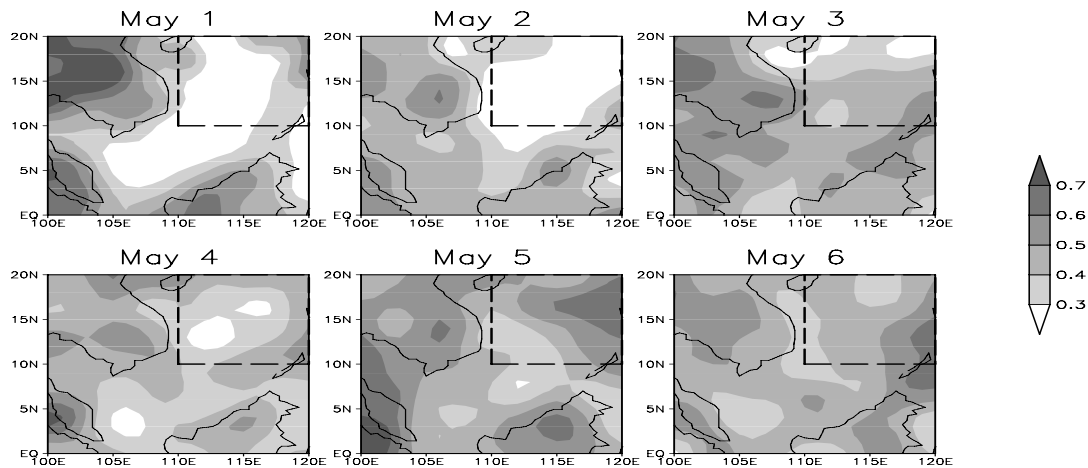


**Figure 1.** Horizontal distribution of the 1998-2006 averaged convective precipitation rate over the SCS for each pentad in May. Unit: mm/h. The rectangular region indicated with dashed lines gives the chosen research area.

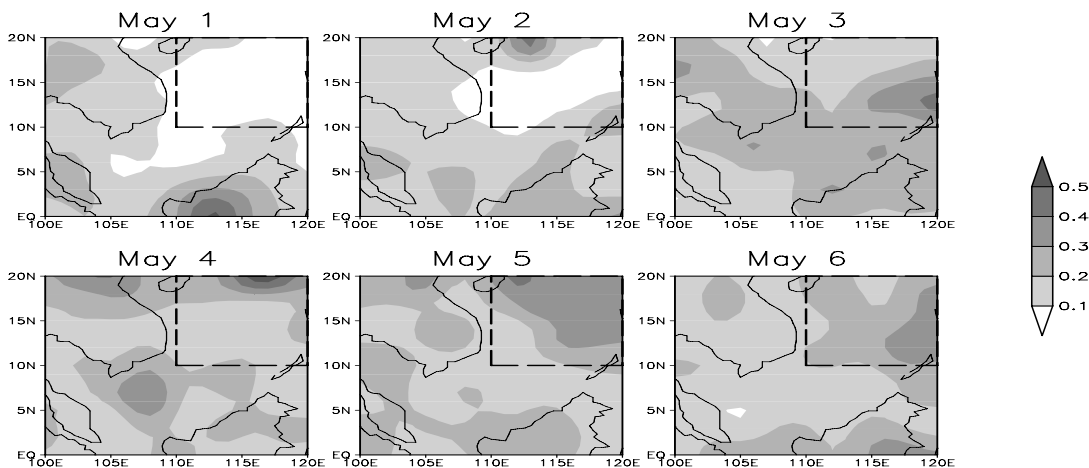


**Figure 2.** Same as Figure 1 but for stratiform precipitation.

### 3.2 Determination of the monsoon onset date

Figures 1 and 2 also show that an abrupt change occurs during the 3rd pentad of May (27th of a year). However, both observations and modeling studies have shown that ENSO can affect the time of monsoon onset<sup>[22-25]</sup>. During an El Niño year, the SCS summer monsoon starts later, while during a La Niña year, it starts earlier. It is therefore necessary to analyze separately the date of monsoon onset during ENSO events. It is well known that if a sea surface temperature difference of at least 0.5°C between the current and averaged values over the equatorial

Pacific region 150–90°W, 5°S–5°N (also known as the Niño3 region) lasts over six months, the situation is defined as an El Niño event. On the contrary, if a difference of lower than –0.5°C lasts over six months, it is called a La Niña event. Figure 3 gives the Niño3 index. As can be seen, from 1998 to 2006, 1998 and 2002 were El Niño years, 1999 was a La Niña year and other years were normal.

Figure 4 shows the PDFs of convective and stratiform rainfalls for the pentads from April to June (19th to 36th pentads of a year) for normal years, El Niño years and La Niña years, respectively. The

figure gives the percentage of convective and stratiform rainfall for each pentad out of the total rainfall during April to June. In Figure 4a, the dashed and dotted lines represent the PDF average for the periods of 19th to 26th pentads and 27th to 36th pentads. Convective rainfall accounts for 1.8% before the 27th pentad and 8.5% afterwards; stratiform rainfall accounts for 1.1% before the 27th pentad and 9.3% afterwards. It is evident that during normal years both convective and stratiform rainfalls demonstrate an abrupt change at the 27th pentad. Hence the 27th pentad can be determined as the monsoon onset time. However for El Niño years (Figure 4b), both convective and stratiform rainfalls increase abruptly

during the 28th pentad from 1.5% and 0.6% (27th pentad) to 7.8% and 6.9% (28th pentad), respectively. This shows that compared to normal years, the monsoon starts later in El Niño years. For La Niña years, both convective and stratiform rainfalls increase abruptly during the 24th pentad from 0.97% and 0.98% (23rd pentad) to 3.97% and 16.79% (24th pentad), respectively. This shows that the monsoon starts earlier in La Niña years. These results are consistent with Huang et al.<sup>[26]</sup> and Fu et al.<sup>[27]</sup>. The results show that it is feasible to determine monsoon onset dates using the abrupt increase of precipitation amount from TRMM data, and the dates determined this way reflects El Niño and La Niña events well.

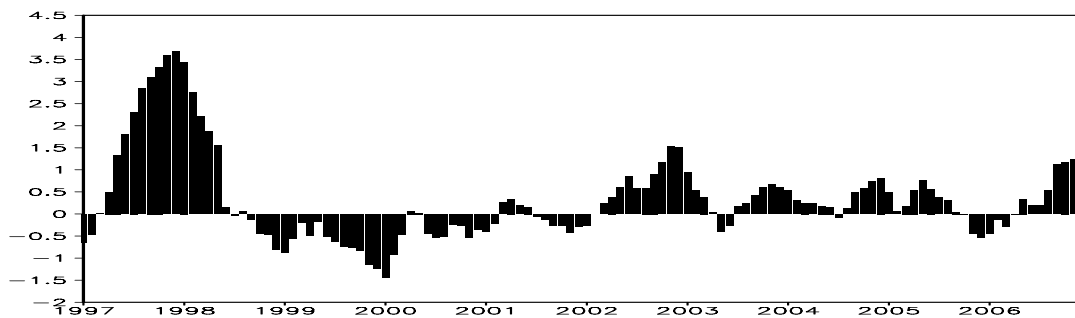


Figure 3. Niño3 index for 1998 to 2006.

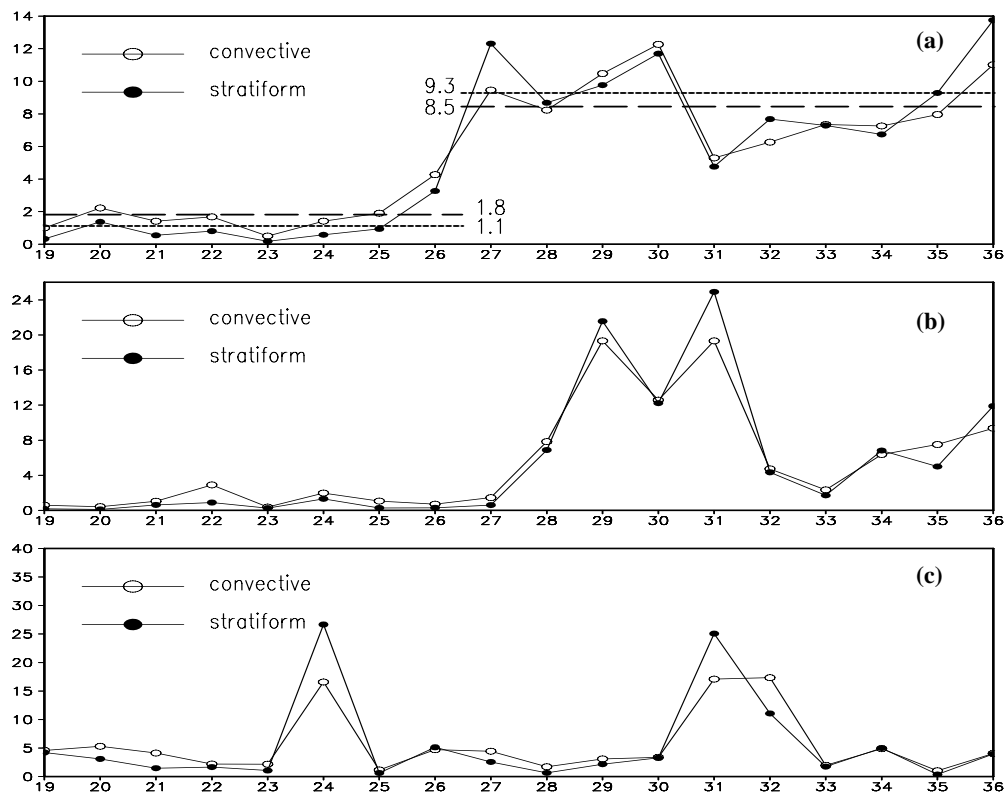


Figure 4. PDFs of convective and stratiform rainfalls for the pentads from April to June for (a) normal years, (b) El Niño years, and (c) La Niña year. X-axis gives the time (pentad) and Y-axis is the percentage.

As shown above, ENSO events have significant impacts on the time of monsoon onset. In this study, we only investigate the precipitation characteristics

before and after monsoon onset for the normal years (2000, 2001, 2003–2006, six years in total). The impact of ENSO events will be discussed in a

subsequent paper.

#### 4 PRECIPITATION CHARACTERISTICS BEFORE AND AFTER MONSOON ONSET

##### 4.1 Comparisons of specific area and specific rainfall

The specific area, defined as the ratio of the number of pixels with certain type of precipitation and the number of total pixels, reflects the probability of this type of precipitation. The specific rainfall is defined as the ratio of the amount of certain type of precipitation to the total amount of precipitation<sup>[25]</sup>.

As shown in Figure 5, the specific areas for both convective and stratiform rainfalls increase significantly after the SCS summer monsoon onset. Before the monsoon onset, the specific areas for the two types of precipitation are very close to each other; after the monsoon onset, the increase in the specific area for the stratiform rain is much larger than that for the convective rain. In other words, before the monsoon onset, the probabilities of both types of rain are about the same, while after the monsoon onset, both of them increase, more evidently with the stratiform rain.

Although the specific area of convective rain is usually smaller than that of the stratiform rain (Figure 5), the specific rainfall of convective rain is usually larger than that of the stratiform rain over the SCS region. Figure 6 shows that before the SCS summer monsoon onset, the specific rainfall for convective rain is about 60%–80%; the specific rainfall for stratiform rain is about 20%–40%. After the summer monsoon onset, however, the specific rainfall for convective rain decreases to 50%–60%. The difference between the specific rainfalls of convective and stratiform rain reduces significantly, even though convective precipitation still has a larger specific rainfall.

##### 4.2 Rainfall strength differences for different rain types before and after the SCS summer monsoon onset

To analyze the changes in rainfall strength before and after the SCS summer monsoon onset, the near-surface rain rate (at 2 km altitude) is categorized into five grades. For the convective rain, the grades are: 0.5–5, 5–10, 10–20, 20–30, and >30 mm/h; for the stratiform rain, they are: 0.5–2, 2–5, 5–10, 10–20, and >20 mm/h. Then the analysis is carried out by comparing the precipitation characteristics for the five pentads before and after the monsoon onset (22nd–26th pentads and 27th–31st pentads).

Figure 7 gives the ratios between observations of the five pentads after monsoon onset and the five pentads before the monsoon onset for the following quantities: the number of precipitation pixels and rainfall amount. As indicated in the figure, the minimum ratio is 2.0 and the maximum is over 10, which demonstrates that after the monsoon onset, both convective and stratiform rainfalls, for both precipitation pixel number and rainfall amount, increase significantly. The stronger the rain is, the larger the ratio. For example, for convective rain rate 0.5–5 mm/h, the ratio is 2.5. If the rain rate is 5–10 mm/h, the ratio becomes 3.1; if the rain rate is 10–20 mm/h, the ratio is 4.2; if the rain rate is 20–30 mm/h, the ratio becomes 6.3; if the rain rate is over 30 mm/h, the ratio becomes 9.4. Comparing Figure 7a with Figure 7b, one can see that the increases in both precipitation pixel number and rainfall amount for stratiform rain are much larger than those for convective rain, which is consistent with Figures 5 and 6, i.e., after the SCS summer monsoon onset, significant enhancements are observed in both convective and stratiform rain, with larger enhancement in stratiform rain.

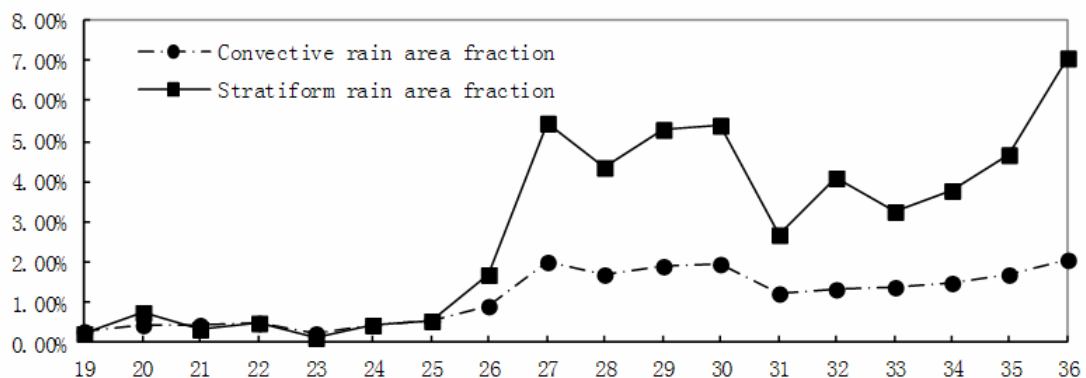


**Figure 5.** The specific areas for convective/stratiform rainfall from 19th pentad to 36th pentad in normal years (no ENSO). X-axis indicates the time; units: pentad.

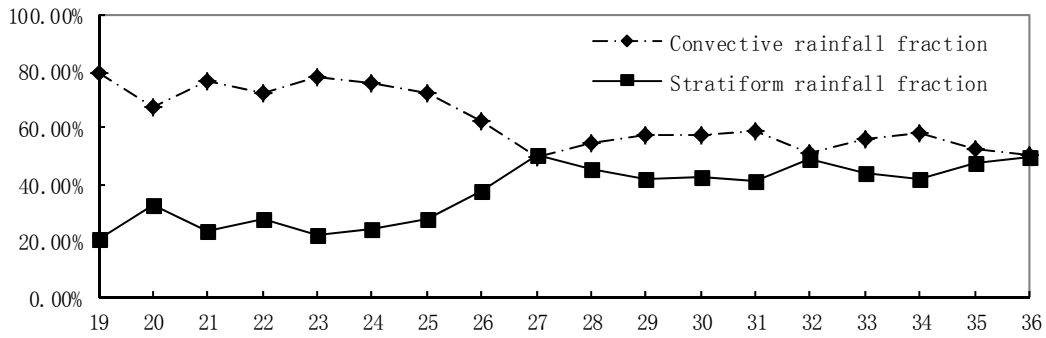


**Figure 6.** The specific rainfalls for convective/stratiform precipitation from 19th pentad to 36th pentad in normal years (no ENSO). X-axis indicates the time; units: pentad.

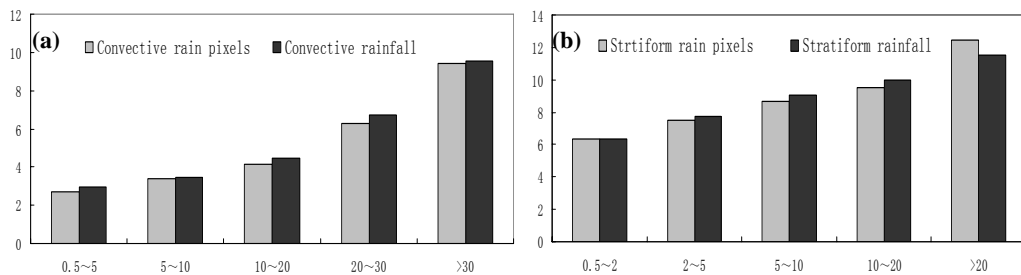


**Figure 7.** The ratio between the precipitation amount after and before monsoon onset. a: convective rain, b: stratiform rain. X-axis indicates the rainrate; units: mm/h.

Figure 8 illustrates the PDF of the number of precipitation pixels and precipitation amount as a function of rainfall strength for both stratiform and convective rain for 22nd–26th pentads and 27th–31st pentads, respectively. As shown in the figure, after the monsoon onset, the percentage of intensive rainfall

increases while that of weak rainfall decreases. On the other hand, the contribution of stratiform rainfall weaker than 5 mm/h decreases after the monsoon onset. For example, stratiform rainfall with strength between 0.5–2 mm/h contributes 29% before the monsoon onset, but only 23% afterwards (Figure 8d).

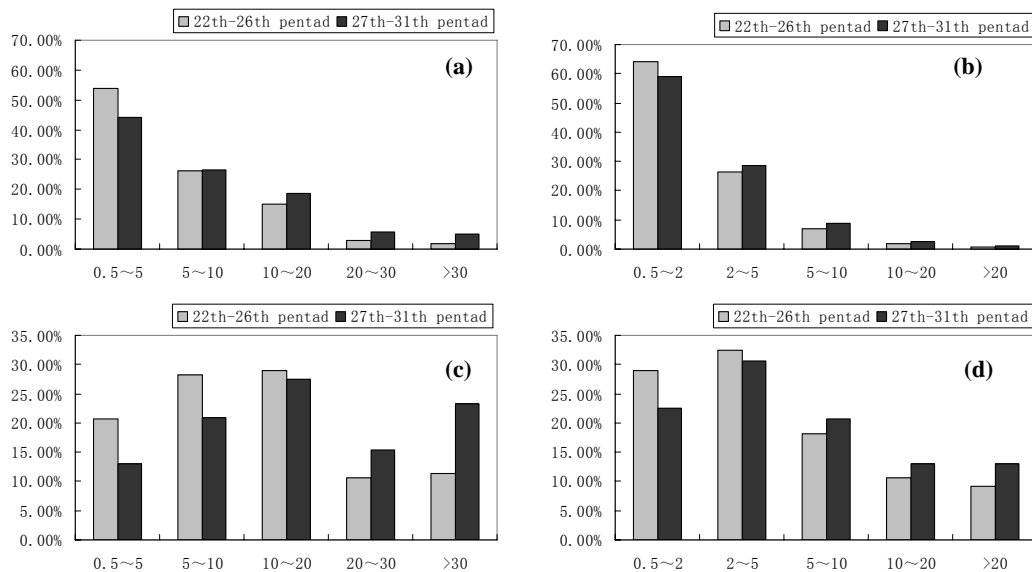


**Figure 8.** The PDFs of convective/stratiform rain before and after the summer monsoon onset as a function of precipitation strength. a: convective rain pixels, b: stratiform rain pixels, c: convective rainfall, d: stratiform rainfall. X-axis indicates rain rate; units: mm/h. Y-axis indicates PDF; units: %.

It is obvious that the precipitation amount is determined by both the number of precipitation pixels

(i.e. precipitation area) and the precipitation strength. A precipitation event with a large area but a small

strength may not result in a large rainfall; on the other hand, if the precipitation strength is large, even it occurs over a relatively small area, the final rainfall amount may be large. For example, during the five pentads before the SCS summer monsoon onset (22nd–26th pentads), even though the area of convective rain rate (0.5–5 mm/h) accounts for the most among all grades (52%, Figure 8a), the rain of this grade does not contribute the most to total rainfall (only 21%, Figure 8c) because of the weaker rain rate. On the contrary, although the convective rain of 10–20 mm/h only accounts for 15% in area (number of pixels), it contributes the most among all rain thresholds (29%). For stratiform rain, the rainfall between 0.5–2 mm/h accounts for the most in terms of number of pixels (64%), but what contributes most to total precipitation is the rainfall between 2–5 mm/h (Figure 8d). Similar results can be seen from the five pentads after the monsoon onset (27th–31st pentads).

#### 4.3 Horizontal distribution of precipitation before

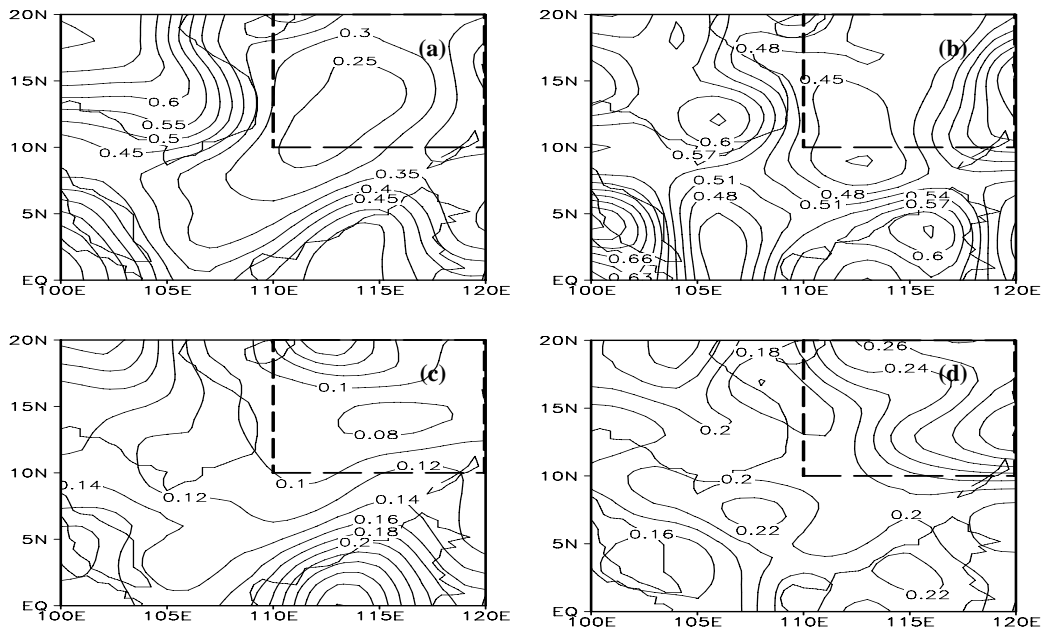


**Figure 9.** Horizontal distribution of average rain rates before (22nd–26th pentads, a, c) and after (27th–31st pentads, b, d); the SCS summer monsoon onset for convective (a, b) and stratiform (c, d) rainfalls.

The onset of the SCS summer monsoon is also a process of adjustment for the atmospheric circulation, which results in evident changes existing in the rain belts before and after the onset. After the establishment of the summer monsoon, the changes in low-level circulations are obvious, manifested by the weakening and northward jump of the cyclonic vortex over the Bay of Bengal. The circulation also changes its pattern from meridional to zonal and extends to the east to the Indochina Peninsula and the northern part of the SCS. As the ridge of the subtropical high recedes toward the east, a branch of strong southwest jet establishes over the eastern part of the Bay of

#### and after the SCS summer monsoon onset

Figure 9 gives the horizontal distribution of precipitation over the SCS region before and after the monsoon onset. It can be seen that the region that changes the most is the central and northern part of the SCS (110–120°E, 10–20°N); the changes over the Indochina Peninsula and the Kalimantan Island are much smaller. Before the monsoon onset, a precipitation minimum is located at the central and northern part of the SCS and the values are 0.25 and 0.08 mm/h for convective and stratiform rainfalls, respectively. After the monsoon onset, however, precipitation increases evidently. The minimum for convective rain moves to the southern part of the SCS and the corresponding value becomes 0.43 mm/h, which is about 1.5 times as much as that before the onset. For stratiform rain, the minimum moves to the northwestern part of the SCS and the corresponding value is about 2.5 times as much as that before the onset.

Bengal, the central and southern part of the Indochina Peninsula and the northern part of the SCS region. At the same time, a monsoon trough is developed over the northern part of the SCS<sup>[28]</sup>. Jointly induced by these factors, the precipitation over the central and northern part of the SCS increases rapidly.

#### 4.4 Differences in vertical structure of precipitation before and after the SCS summer monsoon onset

The vertical change of precipitation rate represents the changing rate of cloud particle sizes as a function of altitude. To a certain extent, it reflects the changes in cloud microphysics and dynamics<sup>[29, 30]</sup>.

As shown in Figure 10, for both the convective and stratiform rain profiles below 4 km, rain rate increases with decrease of altitude; above 6 km, rain rate decreases slowly with height; between 4 and 6 km, the changing rate is bigger. Whether it is before or after

the monsoon onset, the 4 to 6 km layer and the bright band layer are the places where rain rate changes the most for convective and stratiform rainfalls, respectively.

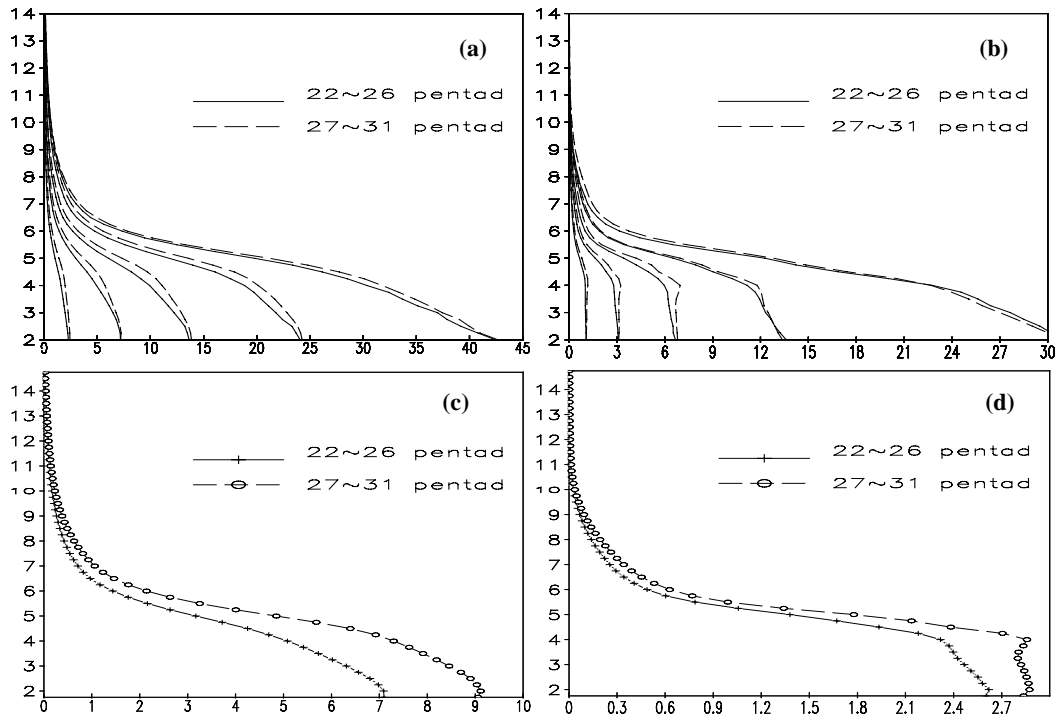


**Figure 10.** Precipitation profiles for convective and stratiform rainfalls over the SCS region. X-axis is the rain rate (mm/h) and Y-axis is the altitude above sea level (km). Panels a and b are the profiles for all five thresholds of rainfall. Panel a (from left to right): 0.5–5, 5–10, 10–20, 20–30, and > 30 mm/h; panel b (from left to right): 0.5–2, 2–5, 5–10, 10–20, and > 20 mm/h. Panels c and d are the profiles of average precipitation for convective and stratiform, respectively.

The smaller/larger the angle between the rain rate profile and horizontal axis, the larger/smaller is the released latent heat. From Figure 10, for both convective and stratiform rainfalls, the angle between the averaged rain rate profile and the horizontal axis is larger for the five pentads before the monsoon onset (22nd–26th pentads), hence less latent heat is released. For the five pentads after the monsoon onset (27th–31st pentads), the angle between the averaged rain rate profile and the horizontal axis is smaller, hence more latent heat is released. These results show that the onset of the SCS summer monsoon is a process of energy release<sup>[16]</sup>, which has significant impact on the atmospheric circulation and energy balance.

Figure 10d shows that after the SCS summer monsoon onset, the change of rain rate below the freezing layer is almost zero, which indicates that the colliding and coalescing process is balanced by the evaporation and breaking processes. Before the monsoon onset, however, the rain rate below the freezing layer increases towards the surface, which indicates that the colliding and coalescing process is stronger than the evaporation and breaking processes. In addition, before the monsoon onset, the stratiform

rain does not show an obvious bright band, but for the five pentads after the onset, a bright band is clearly seen at around 4 km. To study the changes in precipitation vertical structures, the cumulative distribution function (CDF) of the radar reflectivity factor (Z factor) as a function of altitude<sup>[31]</sup> is examined (Figure 11).

We can see that after the monsoon onset, the convective rainfalls become deeper and the near-surface rain rate increases. Take the 99% level for example. Before the monsoon onset, the reflectivity of convective rain at 14 km is 15 dBz, which means at this level the reflectivity bigger than 15 dBz accounts for only 1% of the total rainfall. Similarly, the reflectivity at 2 km is 45 dBz, which means that the reflectivity larger than 45 dBz at 2 km only accounts for 1%. After the monsoon onset, however, the corresponding level (99%) becomes 15 km for 15 dBz, 1 km higher than before. In the same way, the reflectivity at 2 km is 47 dBz, which is larger than before.

Similar results can be seen from the CDFs for stratiform rainfalls (Figures 11c & 11d). Compared to that before the monsoon onset, the stratiform rainfall after the monsoon onset enhances with the level of



freezing layer (bright band) lifted, which probably results from the increased latent heat release after the

monsoon onset.

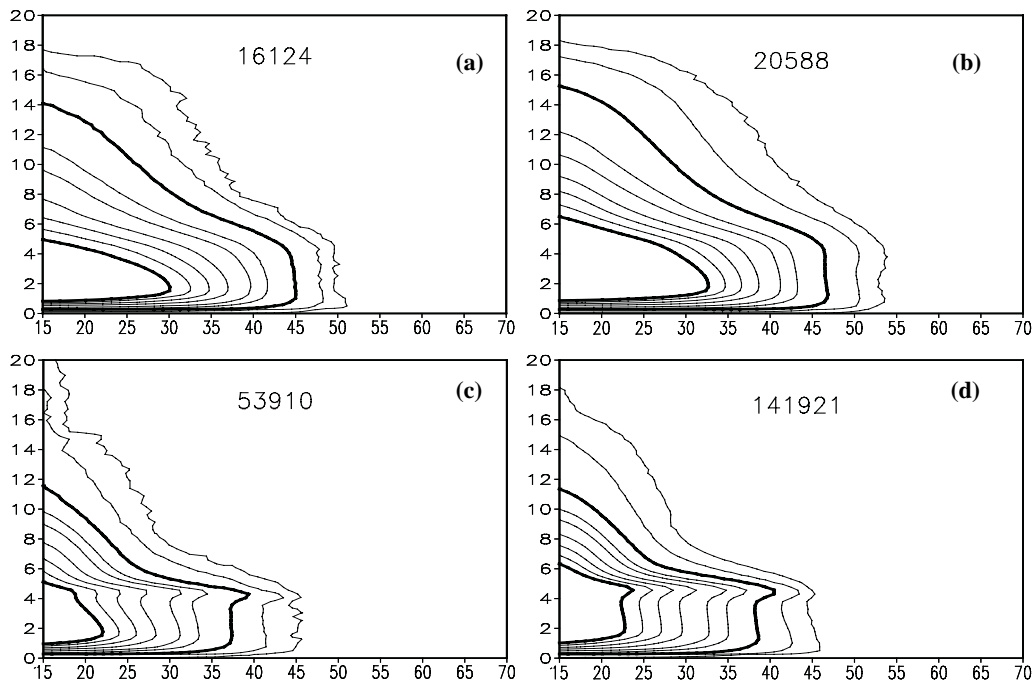


**Figure 11.** The cumulative distribution functions (CDF) of the radar reflectivity factor (Z factor) over the SCS at different altitudes before and after the summer monsoon onset. X-axis: dBz; Y-axis: km. The contour lines are 50% (thick solid line), 60%, 70%, 80%, 90%, 95%, 99% (thick solid line), 99.9% and 99.99%. The integers give the number of samples. a. convective rainfall for the 22nd–26th pentads; b. convective rainfall for the 27nd–31st pentads; c. stratiform rainfall for the 22nd–26th pentads; d. stratiform rainfall for the 27th–31st pentads.

## 5 SUMMARY AND DISCUSSION

The study on the temporal and spatial variations of the precipitation over the area of the SCS during the monsoon onset period shows the points as follows.

(1) The abrupt change in precipitation characteristics before and after the SCS summer monsoon onset is most obvious over the central and northern part of the SCS (110–120°E, 10–20°N). In normal years, the monsoon onset date is the 27th pentad; however it occurs later in El Niño years and earlier in La Niña years.

(2) The precipitation's specific area and specific rainfall show evident differences before and after the monsoon onset. Before the onset, the specific areas for convective and stratiform rainfalls are very close to each other, while after the onset, both specific areas increase significantly, with the increase for stratiform rain being much larger than that for the convective rain. Before the onset, the specific rainfall for the convective precipitation (70%–80%) is much larger than that for the stratiform precipitation (20%–40%). Yet after the monsoon onset, the specific rainfall for the convective precipitation decreases to 50%–60%, while for the stratiform precipitation, it increases to 40%–50%. The differences between the two reduce significantly.

(3) Rainfall of different thresholds demonstrates

different characteristics before and after the onset as well. After the monsoon onset, the percentage of heavy rainfall increases evidently while that of weak rainfall decreases.

(4) After the onset, precipitation increases evidently over the SCS. The minimum for convective rain moves to the southern part of the SCS and the corresponding value is about 1.5 times as much as that before the onset. For stratiform rain, the minimum moves to the northwestern part of the SCS with the minimum about 2.5 times as much as that before the onset.

(5) The vertical structures of the regional rainfall show clear differences before and after the onset. Before/after the onset, the change of rain rate with height is small/large and less/more latent heat is released. The development of summer monsoon results in deeper convection and a higher freezing level over the SCS.

With the TRMM PR radar data, this study takes a step forward towards the understanding of the changes in precipitation characteristics before and after the SCS summer monsoon onset. The impact of summer monsoon on the precipitation is further understood. However, the ambiguous relationship between the precipitation over the SCS region and other circulation systems (i.e., the subtropical high) still needs further investigations.

**Acknowledgement:** The authors would like to express their special gratitude to Dr. YANG Yue-kui (Goddard Earth Science and Technology Center, NASA) for his efforts in translating this thesis from Chinese into English, which has guaranteed the linguistic quality of this thesis.

## REFERENCES:

- [1] DING Yi-hui, LI Chong-yin. The Onset and Evolution of South China Sea Monsoon and Its Interaction with the Ocean [M]. Beijing: China Meteorological Press, 1999: 423.
- [2] CHEN Long-xun, LI Wei, ZHAO Ping, et al. On the process of summer monsoon onset over East Asia [J]. *Clim. Environ. Res.*, 2000, 5(4): 345-355.
- [3] WU Shang-sen, LIANG Jian-yin, LI Chun-hui. Relationship between the intensity of South China Sea Summer Monsoon and the precipitation in raining seasons in China [J]. *J. Trop. Meteor.*, 2003, 19(suppl.): 25-36.
- [4] LAU M K, YANG S. Climatology and interannual variability of the Southeast Asia Summer Monsoon [J]. *Adv. Atmos. Sci.*, 1997, 14(2): 141-161.
- [5] FU Yun-fei, YU Ru-cong, CUI Chun-guang, et al. The structure characteristics of precipitating clouds over the East Asia based on TRMM measurements [J]. *Torrent. Rain and Disast.*, 2007, 26(1): 9-20.
- [6] HOUZE R A. Structure of atmospheric precipitation system: A global survey [J]. *Radio Sci.*, 1981, 16(5): 671-689.
- [7] SZOKE E J, ZIPSER E J, JORGENSEN D P. A radar study of convective cells in mesoscale systems in GATE, Part I: Vertical profiles statistics and comparison with hurricanes [J]. *J. Atmos. Sci.*, 1986, 43(2): 182-197.
- [8] HOBBS P V. Research on clouds and precipitation past, present, and future [J]. *Bull. Amer. Meteor. Soc.*, 1989, 70(3): 282-285.
- [9] HOUZE R A. Stratiform precipitation in regions of convection: A meteorological paradox? [J]. *Bull. Amer. Meteor. Soc.*, 1997, 78(10): 2179-2196.
- [10] YAN Jun-yue, TANG Zhi-yi, YAO Hua-dong, et al. A synoptic study on establishment of the monsoon and associated variation of rain belt over the South China Sea in 2002 [J]. *Acta Meteor. Sinica*, 2003, 61(5): 569-579.
- [11] JIANG Jing, QIAN Yong-fu. The general character of precipitation over the South China Sea [J]. *Acta Meteor. Sinica*, 2000, 58(1): 60-69.
- [12] LIU Yan-ju, DING Yi-hui, ZHAO Nan. A study on the meso-scale convective systems during summer monsoon onset over the South China Sea in 1998. Part I: Analysis of large-scale fields for occurrence and development of meso-scale convective systems [J]. *Acta Meteor. Sinica*, 2005, 63(4): 431-442.
- [13] FU Yun-fei, LIN Yi-hua, LIU Guo-sheng, et al. Seasonal characteristics of precipitation in 1998 over East Asia as derived from TRMM PR [J]. *Adv. Atmos. Sci.*, 2003, 20(4): 511-529.
- [14] JIN Zhu-hui, TAO Shi-yan. The onset of the summer monsoon over the South China Sea and its active and break periods [J]. *Clim. Environ. Res.*, 2002, 7(3): 267-278.
- [15] DING Yi-hui, LI Chong-yin, HE Jin-hai. South China Sea Monsoon Experiment (SCSMEX) and the East-Asian Monsoon [J]. *Acta Meteor. Sinica*, 2004, 62(5): 561-586.
- [16] LIANG Bi-qi. The Tropical Atmospheric Circulation over South China Sea [M]. Beijing: China Meteorological Press, 1991: 11-15.
- [17] TAO Shi-yan, CHEN Long-xun. A Review of Recent Research on the East Asian Summer Monsoon in China [M]//*Monsoon Meteorology*, Oxford: Oxford University Press, 1987: 60-92.
- [18] HE Jin-hai, ZHU Qian-gen, MURAKAMI M. TBB data revealed features of Asian Australian Monsoon seasonal transition and Asian Summer Monsoon establishment [J]. *J. Trop. Meteor.*, 1996, 12(1): 34-42.
- [19] LUO Hui-bang. The Onset of South China Sea Monsoon and Its Rain Belt Evolution [M]. Beijing: China Meteorological Press, 1999: 25-29.
- [20] QIAO Yun-ting, JIAN Mao-qiu, LUO Hui-bang. Different characteristics of precipitation over four sub-regions of South China Sea during summer monsoon and the abrupt change [J]. *J. Trop. Meteor.*, 2002, 18(1): 38-44.
- [21] LI Chun-hui, LIANG Jian-yin. A review of activities of summer monsoon over South China Sea in 2004 [J]. *J. Trop. Meteor.*, 2005, 21(6): 561-569.
- [22] HUANG Rong-hui, CHEN Wen, DING Yi-hui, et al. Studies on the monsoon dynamics and the interaction between monsoon and ENSO cycle [J]. *Chin. J. Atmos. Sci.*, 2003, 27(4): 484-502.
- [23] CHEN Long-xun, LIU Hong-qing, WANG Wen, et al. Preliminary study on the characteristics and mechanism of summer monsoon onset over South China Sea and region adjacent to it [J]. *Acta Meteor. Sinica*, 1999, 57(1): 16-29.
- [24] LIANG Jian-yin, WU Shang-sen, YOU Ji-ping. The research on variations of onset time of the SCS summer monsoon and its intensity [J]. *J. Trop. Meteor.*, 1999, 15(2): 97-105.
- [25] YAN Jun-yue. Climatological characteristics on the onset of the South China Sea Southwest Monsoon [J]. *Acta Meteor. Sinica*, 1997, 55(2): 174-186.
- [26] HUANG Rong-hui, GU Lei, XU Yu-hong, et al. Characteristics of the interannual variations of onset and advance of the East Asian Summer Monsoon and their associations with thermal states of the Tropical Western Pacific [J]. *Chin. J. Atmos. Sci.*, 2005, 29(1): 20-36.
- [27] LI Rui, FU Yun-fei, ZHAO Ping. Characteristics of rainfall structure over the tropical pacific during the later period of 1997/1998 El Nino derived from TRMM PR observations [J]. *Chin. J. Atmos. Sci.*, 2005, 29(2): 225-235.
- [28] The PLA General Staff Meteorological Administration. The Weather, Military Meteorological and Hydrological Forecast of South China Sea [M]. Beijing: People's Liberation Army Press, 1996: 56-57.
- [29] LIU G, TAKEDA T. Two types of stratiform precipitating clouds associated with cyclones [J]. *Tenki*, 1989, 36: 147-157.
- [30] ZIPSER E J, LUTZ K R. The vertical profile of radar reflectivity of convective cells: A strong indicator of storm intensity and lightning probability? [J]. *Mon. Wea. Rev.*, 1994, 122(8): 1751-1759.
- [31] CECIL D J, ZIPSER E J, NESBITT S W. Reflectivity, ice scattering, and lightning characteristics of hurricane eyewalls and rainbands. Part I: Quantitative description [J]. *Mon. Wea. Rev.*, 2002, 130(4): 769-784.

**Citation:** LI Yao-dong, SONG Ming-kun and HU Liang. A study on the precipitation characteristics over the South China Sea before and after the monsoon onset. *J. Trop. Meteor.*, 2012, 18(1): 1-10.